Application of Singular Eigenfunction Expansions to the Propagation of Periodic Disturbances in a Radiating Grey Gas

PING CHENG*
Ames Research Center, National Aeronautics and Space Administration, Moffett Field, California 94035
AND
A. LEONARD
Department of Mechanical Engineering, Stanford University, Stanford, California 94305
(Received 10 November 1969; final manuscript received 6 July 1970)

The effect of thermal radiation on the propagation of small disturbances generated by the harmonic oscillation of a planar wall, either in position or temperature or both, is considered. By separation of variables, it is shown that the governing linearized equations can be reduced to a homogeneous integral equation that admits both regular and singular solutions to form a complete set; thus, the problem can be solved by the application of singular eigenfunction expansions analogous to those used in neutron-transport theory. An exact closed form solution is obtained for disturbed quantities in the flow and radiation fields. The exact solution shows that the disturbances consist of a damped continuum mode with infinite wave speed in addition to two discrete modes with finite wave speed. One of the discrete modes represents the "modified classical" wave whereas the other discrete mode plus the continuum mode corresponds to the radiation-induced wave. For sufficiently small Bouguer numbers, the discrete mode of the radiation-induced wave disappears. The newly found continuum mode damps faster than the discrete mode. Consequently, only the discrete modes persist away from the boundary. The differential approximation is found to predict the modified classical wave accurately but predicts the radiation-induced wave only approximately. The implications as well as the accuracy of the differential approximation are discussed and compared.

I. INTRODUCTION

The problem of propagation of small disturbances generated by the harmonic oscillation of a planar wall, either in position or temperature or both, has been studied by a number of investigators. In particular, a comprehensive study was made by Vincenti and Baldwin,[1] who solved the governing integrodifferential equation by the so-called exponential approximation. The results show that a modified classical wave and a radiation-induced wave, with different wave speeds and damping factors, exist in the flow field. Later, Cheng[2] reconsidered the same problem based on the differential approximation,[2–6] which is essentially the first approximation of the more systematic spherical-harmonic method in neutron-transport theory. It was concluded by Cheng[2] that the differential approximation with Mark's boundary condition is mathematically equivalent to the exponential approximation if coefficients of the exponential function are properly chosen. Thus, the gross features of the physical phenomena of the problem and the mathematical basis of the approximation of the solution are understood although the accuracy of the approximation involved is not well known.

Recently, a number of papers[7–9] have appeared to assess the accuracy of the approximation by comparing results based on the differential approximation to that of direct numerical integration of the nonlinear integrodifferential equations in some planar problems in radiative gasdynamics. Nevertheless, the truncation error and the step size of the numerical integration undoubtedly influence the accuracy of the results and only qualitative comparison is possible. In order to assess the accuracy of the differential approximation for a given geometry, it is therefore desirable to obtain an exact analytic solution with which results based on that of differential approximation can be quantitatively compared.

Case[10] has developed a new method to obtain an exact analytic solution to the one-speed integrodifferential equation for neutron transport in plane geometry. A number of problems previously solved approximately in neutron-transport theory have been re-examined using this technique.[11] Since the governing integrodifferential equation for radiative transport in a grey gas is essentially the same equation as that of one-speed neutron transport, the method has been extended to solve problems in radiative equilibrium.[12,13] In radiative gasdynamics where the radiation field is interacting with the flow field, the effect of scattering is usually neglected; the integrodifferential equation arises, not from the radiation-transport equation, but from the energy equation.[14] It would appear from the outset that the mathematical difficulties of problems in radiative gasdynamics and neutron transport are somewhat different. Nevertheless, the spherical harmonic method has been proved useful in both of these disciplines.[2,5] It will be shown that the set of linearized equations for planar radiative gasdynamics have essentially the same mathematical features as the integrodifferential equation of neutron transport in planar geometry.

The problem considered in this paper is the same as that considered by Vincenti and Baldwin.[1] By means of separation of variables, it is shown that the set of integrodifferential equations can be reduced to a homogeneous integral equation similar to that in neutron-transport theory. An exact closed-form solution can be obtained as the superposition of singular and regular solutions analogous to the problem of neutron transport

in a half-space that has been considered by Case.[11] As far as the authors are aware, this is the first exact analytic solution obtained in radiative gasdynamics in the presence of a radiating wall.

The results show that infinitely many waves with different damping constants and wave speeds exist. In general, these waves consist of two discrete modes with finite wave speeds and a continuum mode with an infinite wave speed. The exact solution shows that the modified classical wave is represented by one of the discrete modes, whereas the radiation-induced wave consists of the other discrete mode plus the continuum mode. The discrete mode of the radiation-induced wave disappears for sufficiently small Bouguer numbers (i.e., for small absorption coefficient of the gas or high-frequency oscillation of the wall). The newly found continuum mode damps faster than the discrete mode; consequently, only the discrete mode persists away from the boundary. Physically, the discrete mode represents the diffusionlike behavior which is isotropic in nature, whereas the continuum mode takes care of the nonisotropic character of the radiation field, which is important for small Bouguer numbers and near the boundary. The numerical values of disturbances at the gas–solid interface as obtained from the exact solution and the differential approximation are compared.

Although exact two- and three-dimensional solutions to analogous problems seem to be out of reach at this time, recent developments[15] in the analysis of one-dimensional spherically symmetric problems in transport theory indicate that propagation of small spherically symmetric disturbances generated by a sphere could also be analyzed exactly. Similar results in cylindrical geometry, however, do not exist at this time.

II. REDUCTION TO AN INTEGRAL EQUATION

We now consider the problem of small disturbances propagating into a uniform medium at rest. The linearized equations of state and radiation transport yield

$$\frac{\partial}{\partial t}\left(\mu\frac{\partial}{\partial x}+\alpha_\infty\right)I'=-\frac{4\alpha_\infty\sigma T_\infty{}^3}{\pi R}\left(\frac{\partial^2}{\partial t^2}-a_T{}^2\frac{\partial^2}{\partial x^2}\right)\phi. \quad (1)$$

With the aid of Eq. (1), the linearized equations of continuity, momentum, and energy can be combined to give

$$\frac{\partial}{\partial t}\left(\frac{\partial^2}{\partial t^2}-a_s{}^2\frac{\partial^2}{\partial x^2}\right)\phi+\frac{16\gamma a_s\alpha_\infty}{\mathrm{Bo}}\left(\frac{\partial^2}{\partial t^2}-a_T{}^2\frac{\partial^2}{\partial x^2}\right)\phi$$
$$=-\frac{2\pi\alpha_\infty(\gamma-1)}{\rho_\infty}\int_{-1}^{1}\frac{\partial I'}{\partial t}(x,\mu,t)\,d\mu, \quad (2)$$

where the disturbance potential is defined by $u'=\partial\phi/\partial x$ and $p'=-\rho_\infty\partial\phi/\partial t$, with u' and p' denoting the disturbed velocity and pressure, $a_s=(\gamma RT_\infty)^{1/2}$ and $a_T=(RT_\infty)^{1/2}$ are the isentropic and the isothermal speeds of sound, $\mathrm{Bo}\equiv\rho_\infty a_s R\gamma/[(\gamma-1)\sigma T_\infty{}^3]$ is the Boltzmann number, and γ and R are the specific heat ratio and the gas constant. The quantities σ and α_∞ are, respectively, the Stefan–Boltzmann constant and the absorption coefficient with the subscript ∞ denoting the undisturbed condition which is uniform and isotropic. Also, $\mu\equiv\cos\theta$ where θ is the angle between the direction of propagation of radiation intensity and the positive x axis. Equation (1) and (2) are the two governing equations for the unknowns ϕ and I'.

For the specific problem of disturbances generated by harmonic oscillation of a planar wall, either in position or temperature or both, the boundary conditions are

$$u'(0,t)=\frac{\partial\phi}{\partial x}(0,t)=R\frac{T_\infty}{a_s}A\exp(i\omega t), \quad (3)$$

and

$$\frac{\partial T_w'}{\partial t}(t)=\omega T_\infty B\exp(i\omega t), \quad (4a)$$

where ω is the frequency of oscillation, and A and B are dimensionless constants to be given. If the wall is assumed to be black, boundary condition (4a) can be rewritten in terms of I' as

$$\frac{\partial I'}{\partial t}(0,\mu,t)=\frac{4\sigma T_\infty{}^4}{\pi}\omega B\exp(i\omega t), \qquad 0<\mu<1. \quad (4b)$$

At infinity, ϕ is bounded and I' vanishes.

Boundary conditions (3) and (4) and the translation invariance of the governing equations suggest that the solution is of the form

$$\phi=(RT_\infty/\omega)C_\nu\exp[-(\xi/\nu)+i\omega t], \quad (5)$$

and

$$\frac{\partial I'}{\partial t}=\frac{4\sigma T_\infty{}^4\omega}{\pi}A_\nu\exp\left(-\frac{\xi}{\nu}+i\omega t\right)\Psi_\nu(\mu), \quad (6)$$

where $\xi=\omega x/a_s$ is a dimensionless independent variable, C_ν and A_ν are dimensionless (real or complex) constants to be determined, and $\Psi_\nu(\mu)$ is a function of μ associated with eigenvalue ν, also to be determined. We now search for values of ν which admit nontrivial solutions.

The substitution of Eqs. (5) and (6) into Eqs. (1) and (2) leads to

$$\left(1-\frac{\mu}{\mathrm{Bu}\nu}\right)\Psi_\nu(\mu)=\frac{1}{2g(\nu)}\int_{-1}^{1}\Psi_\nu(\mu')\,d\mu', \quad (7)$$

where

$$g(\nu)=(1+i\beta)(\nu^2-\zeta^2)/(\nu^2+\gamma^{-1}),$$

with $\beta\equiv\mathrm{Bo}/16\gamma\mathrm{Bu}$, $\zeta^2\equiv-[(1/\gamma)+i\beta](1+i\beta)^{-1}$, and $\mathrm{Bu}\equiv\alpha_\infty a_s/\omega$ denoting the Bouguer number. Equation (7) is an integral equation for the function $\Psi_\nu(\mu)$.

III. EXACT SOLUTION BY THE METHOD OF SINGULAR EIGENFUNCTION EXPANSIONS

Equation (7) is similar to the integral equation considered by Case[11] in problems connected with neutron-

transport theory. The analysis of the present problem can then proceed in an analogous way.

Since Eq. (7) is a homogeneous equation for $\Psi_\nu(\mu)$ and the integral on the right-hand side of Eq. (7) is a numerical constant, we can normalize the function $\Psi_\nu(\mu)$ such that

$$\int_{-1}^{1} \Psi_\nu(\mu)\, d\mu = 1. \tag{8}$$

With the normalization condition, Eq. (7) becomes

$$[\mathrm{Bu}\nu - \mu]\Psi_\nu(\mu) = \mathrm{Bu}\nu/2g(\nu), \qquad -1 \le \mu \le 1. \tag{9}$$

The solution of Eq. (9) for $\Psi_\nu(\mu)$ depends on the value of ν. There are two possibilities.

(i) If the value of ν does not lie on the real line between the interval $(-1/\mathrm{Bu}, 1/\mathrm{Bu})$, Eq. (9) can be solved to give

$$\Psi_\nu(\mu) = \mathrm{Bu}\nu/[2g(\nu)\,(\mathrm{Bu}\nu - \mu)], \tag{10}$$

which if inserted into the normalization condition (8) gives

$$\Lambda(\nu) \equiv 1 - \frac{\mathrm{Bu}\nu}{2g(\nu)} \int_{-1}^{1} \frac{d\mu}{\mathrm{Bu}\nu - \mu} = 1 - \frac{\mathrm{Bu}\nu}{2g(\nu)} \ln \frac{\mathrm{Bu}\nu + 1}{\mathrm{Bu}\nu - 1} = 0. \tag{11}$$

Equation (11) is a transcendental equation for the determination of the eigenvalues ν. It is shown in Appendix A that Eq. (11) has four roots if $\beta \le \beta_c$ and has two roots if $\beta > \beta_c$. Since the function $\Lambda(\nu)$ is an even function, we can write these roots as $\pm\nu_j$ ($j = 0, 1$ for $\beta \le \beta_c$ and $j = 0$ for $\beta > \beta_c$). For the case when $\mathrm{Bu} \gg 1$, the logarithmic term in Eq. (11) can be expanded in power series in $1/\mathrm{Bu}$, and, if the first two terms in the infinite series are retained, the dispersion relation obtained by Vincenti and Baldwin[1] and by Cheng[2] is recovered.

It is worth noting that the exact dispersion function, Eq. (11) has poles at $\nu = \pm\zeta$, a branch cut along the real line from $-1/\mathrm{Bu}$ to $1/\mathrm{Bu}$ and is analytic elsewhere. It follows from the Plemelj formulas[16] that for ν on the cut,

$$\Lambda^{\pm}(\nu) = 1 - \frac{\mathrm{Bu}\nu}{2g(\nu)} P \int_{-1}^{1} \frac{d\mu}{\mathrm{Bu}\nu - \mu} \pm \frac{\pi i \mathrm{Bu}\nu}{2g(\nu)}$$

$$= 1 - \frac{\mathrm{Bu}\nu}{2g(\nu)} \ln \frac{1 + \mathrm{Bu}\nu}{1 - \mathrm{Bu}\nu} \pm \frac{\pi i \mathrm{Bu}\nu}{2g(\nu)}, \tag{12}$$

where P denotes the principal value of the integral and $\Lambda^{\pm}(\nu)$ are the boundary values of $\Lambda(\nu)$ along the branch cut when ν approaches from the upper $(+)$ and the lower $(-)$ side of the cut.

(ii) If ν lies on the real line in the interval $(-1/\mathrm{Bu}, 1/\mathrm{Bu})$, the solution of Eq. (9) is given by

$$\Psi_\nu(\mu) = [\mathrm{Bu}\nu/2g(\nu)]P[1/(\mathrm{Bu}\nu - \mu)] + \lambda(\nu)\,\delta(\mathrm{Bu}\nu - \mu), \tag{13}$$

where the δ-function term contribution represents the homogeneous solution of Eq. (9). The function $\lambda(\nu)$ is obtained by substituting Eq. (13) into the normalization condition (8) to yield

$$\lambda(\nu) = 1 - [\mathrm{Bu}\nu/2g(\nu)] \ln[(1 + \mathrm{Bu}\nu)/(1 - \mathrm{Bu}\nu)]. \tag{14}$$

Since $\lambda(\nu)$ can always be chosen such that Eq. (14) is satisfied, any value of ν in the interval $(-1/\mathrm{Bu}, 1/\mathrm{Bu})$ is an acceptable eigenvalue. It follows from Eqs. (12) and (14) that

$$\Lambda^{+}(\nu) - \Lambda^{-}(\nu) = \pi i \mathrm{Bu}\nu/g(\nu), \tag{15a}$$

$$\Lambda^{+}(\nu) + \Lambda^{-}(\nu) = 2\lambda(\nu), \tag{15b}$$

and

$$\Lambda^{\pm}(\nu) = \lambda(\nu) \pm \pi i \mathrm{Bu}\nu/2g(\nu). \tag{15c}$$

Thus, we have found that in addition to the discrete eigenvalues ν_j with associated eigenfunctions Ψ_{ν_j}, there is a continuum of eigenvalues in the interval $(-1/\mathrm{Bu}, 1/\mathrm{Bu})$ with associated eigenfunctions given by Eq. (13). We now assume that the solution can be written as a superposition of these eigenfunctions each multiplied by the corresponding exponential in the spatial variable according to Eq. (6). Thus, we have

$$\frac{\partial I'}{\partial t}(\xi, \mu, t) = \frac{4\sigma T_\infty{}^4 \omega}{\pi} \left\{ a_{0+} \exp\left(-\frac{\xi}{\nu_0}\right) \Psi_{\nu_0}(\mu) + a_{0-} \exp\left(\frac{\xi}{\nu_0}\right) \Psi_{-\nu_0}(\mu) + k \left[a_{1+} \exp\left(-\frac{\xi}{\nu_1}\right) \Psi_{\nu_1}(\mu) + a_{1-} \exp\left(\frac{\xi}{\nu_1}\right) \Psi_{-\nu_1}(\mu) \right] + \int_{-1/\mathrm{Bu}}^{1/\mathrm{Bu}} A(\nu) \times \exp\left(-\frac{\xi}{\nu}\right) \Psi_\nu(\mu)\, d\nu \right\} \exp(i\omega t), \tag{16}$$

where

$$k \equiv \frac{[\theta_1(1/\mathrm{Bu}) - \theta_1(-1/\mathrm{Bu})]}{2\pi},$$

which is introduced so that the terms in the square bracket vanish for $\beta > \beta_c$ ($k = 1$ for $\beta \le \beta_c$ and $k = 0$ for $\beta > \beta_c$). According to Eq. (5) and with the aid of Eqs. (6), (1), and (8), we have the following expansion for ϕ:

$$\phi(\xi, t) = \frac{RT_\infty}{\omega} \left\{ \frac{1}{2g(\nu_0)[1 + (1/\gamma\nu_0{}^2)]} \left[a_{0+} \exp\left(-\frac{\xi}{\nu_0}\right) + a_{0-} \exp\left(\frac{\xi}{\nu_0}\right) \right] + \frac{k}{2g(\nu_1)[1 + (1/\gamma\nu_1{}^2)]} \times \left[a_{1+} \exp\left(-\frac{\xi}{\nu_1}\right) + a_{1-} \exp\left(\frac{\xi}{\nu_1}\right) \right] + \int_{-1/\mathrm{Bu}}^{1/\mathrm{Bu}} \frac{A(\nu) \exp(-\xi/\nu)\, d\nu}{2g(\nu)[1 + (1/\gamma\nu^2)]} \right\} \exp(i\omega t). \tag{17}$$

The remaining task is to show that the coefficients $a_{0\pm}$, $a_{1\pm}$, and $A(\nu)$ may be determined uniquely and to obtain expressions for these coefficients.

Since the disturbances are bounded at infinity, the coefficients associated with eigenvalues with negative real part must vanish, i.e., $a_{0-}=a_{1-}=0$ and $A(\nu)=0$ for $\nu<0$. With this consideration, the average radiation intensity is given by

$$\frac{\partial I_0'}{\partial t}(\xi,t)=2\pi\int_{-1}^{1}\frac{\partial I'}{\partial t}(\xi,\mu,t)\,d\mu$$

$$=8\sigma T_\infty^4\omega\left[a_{0+}\exp\left(-\frac{\xi}{\nu_0}\right)+ka_{1+}\exp\left(-\frac{\xi}{\nu_1}\right)\right.$$

$$\left.+\int_0^{1/\mathrm{Bu}}A(\nu)\exp\left(-\frac{\xi}{\nu}\right)d\nu\right]\exp(i\omega t), \quad (18)$$

and the radiative heat flux is given by

$$\frac{\partial q'}{\partial t}(\xi,t)=8\sigma T_\infty^4\omega\,\mathrm{Bu}\left[a_{0+}\nu_0\left(1-\frac{1}{g(\nu_0)}\right)\exp\left(-\frac{\xi}{\nu_0}\right)\right.$$

$$+ka_{1+}\nu_1\left(1-\frac{1}{g(\nu_1)}\right)\exp\left(-\frac{\xi}{\nu_1}\right)$$

$$\left.-\int_0^{1/\mathrm{Bu}}\nu A(\nu)\left(1-\frac{1}{g(\nu)}\right)\exp\left(-\frac{\xi}{\nu}\right)d\nu\right]\exp(i\omega t), \quad (19)$$

where we have made use of Eq. (16). The disturbed velocity, pressure, etc., in the flow field can be obtained by appropriate differentiation of Eq. (17).

We now determine the coefficients a_{0+}, a_{1+}, and $A(\nu)$ by first imposing the radiative boundary condition (4b) and the condition at infinity on Eq. (16) to give

$$\Psi'(\mu)=\int_0^{1/\mathrm{Bu}}A(\nu)\Psi_\nu(\mu)\,d\nu, \qquad 0<\mu<1, \quad (20a)$$

where

$$\Psi'(\mu)\equiv B-a_{0+}\Psi_{\nu_0}(\mu)-ka_{1+}\Psi_{\nu_1}(\mu). \quad (20b)$$

Substitution of Eq. (13) into Eq. (20a) yields

$$\mathrm{Bu}\Psi'(\mathrm{Bu}\tilde{\mu})=\lambda(\tilde{\mu})A(\tilde{\mu})+P\int_0^{1/\mathrm{Bu}}\frac{\mathrm{Bu}\nu A(\nu)\,d\nu}{2g(\nu)(\nu-\tilde{\mu})},$$

$$0<\tilde{\mu}<1/\mathrm{Bu}, \quad (21)$$

where $\tilde{\mu}\equiv\mu/\mathrm{Bu}$. Equation (21) is a singular integral equation for $A(\nu)$. To solve for $A(\nu)$, we first introduce a function $n(z)$ such that

$$n(z)=\frac{1}{2\pi i}\int_0^{1/\mathrm{Bu}}\frac{\mathrm{Bu}\nu A(\nu)\,d\nu}{2g(\nu)(\nu-z)}. \quad (22)$$

If we assume that $A(\nu)/g(\nu)$ is sufficiently well-behaved, the function $n(z)$ has the following properties:

(i) $n(z)$ is analytic in the complex plane cut from 0 to $1/\mathrm{Bu}$ along the real line.

(ii) It goes to zero at least as fast as $1/z$ at infinity. With the aid of the Plemelj formulas, it follows from Eq. (22) that

$$n^+(\tilde{\mu})+n^-(\tilde{\mu})=\frac{1}{\pi i}P\int_0^{1/\mathrm{Bu}}\frac{\mathrm{Bu}\nu A(\nu)\,d\nu}{2g(\mu)(\nu-\tilde{\mu})},$$

$$0<\tilde{\mu}<1/\mathrm{Bu}, \quad (23a)$$

and

$$n^+(\tilde{\mu})-n^-(\tilde{\mu})=\mathrm{Bu}\tilde{\mu}A(\tilde{\mu})/2g(\tilde{\mu}). \quad (23b)$$

Equation (21), with the aid of Eqs. (23) and (15c), can be written in the form

$$\Lambda^+(\tilde{\mu})n^+(\tilde{\mu})-\Lambda^-(\tilde{\mu})n^-(\tilde{\mu})=[\mathrm{Bu}^2\tilde{\mu}/2g(\tilde{\mu})]\Psi'(\mathrm{Bu}\tilde{\mu}),$$

$$0\leq\tilde{\mu}\leq1/\mathrm{Bu}. \quad (24)$$

It should be noted that the function $\Lambda(z)$ has a branch cut between 0 and $1/\mathrm{Bu}$. To solve Eq. (24), we introduce a function $X(z)$ such that

$$X^+(\tilde{\mu})/X^-(\tilde{\mu})=\Lambda^+(\tilde{\mu})/\Lambda^-(\tilde{\mu}), \qquad 0\leq\tilde{\mu}\leq1/\mathrm{Bu}, \quad (25)$$

and with the additional properties: (i) $X(z)$ is analytic in the complex plane cut from 0 to $1/\mathrm{Bu}$. (ii) $X(z)$ is nonzero in the finite plane.

It is shown in Appendix B that the function satisfying relation (25) with properties (i) and (ii) is

$$X(z)=\frac{1}{(1-\mathrm{Bu}z)^k}\times\exp\left[\frac{1}{2\pi i}\int_0^{1/\mathrm{Bu}}\ln\left(\frac{\Lambda^+(\tilde{\mu})}{\Lambda^-(\tilde{\mu})}\right)\frac{d\tilde{\mu}}{\tilde{\mu}-z}\right]. \quad (26)$$

The determination of $X(z)$ is unique up to a constant multiple.

With the aid of Eq. (25), Eq. (24) can be written as

$$n^+(\tilde{\mu})X^+(\tilde{\mu})-n^-(\tilde{\mu})X^-(\tilde{\mu})=\gamma(\tilde{\mu})\Psi'(\mathrm{Bu}\tilde{\mu}),$$

$$0\leq\tilde{\mu}\leq1/\mathrm{Bu}, \quad (27a)$$

where

$$\gamma(\tilde{\mu})\equiv\frac{\mathrm{Bu}^2\tilde{\mu}X^+(\tilde{\mu})}{2g(\tilde{\mu})\Lambda^+(\tilde{\mu})}=\frac{\mathrm{Bu}}{2\pi i}[X^+(\tilde{\mu})-X^-(\tilde{\mu})]. \quad (27b)$$

With the use of the Plemelj formulas, it is easy to show that $n(z)$ is given by

$$n(z)=\left(\frac{1}{2\pi iX(z)}\right)\int_0^{1/\mathrm{Bu}}\frac{\gamma(\tilde{\mu})\Psi'(\mathrm{Bu}\tilde{\mu})\,d\tilde{\mu}}{\tilde{\mu}-z}, \quad (28)$$

which has boundary values n^+ and n^- that satisfy Eq. (27a). Substitution of Eqs. (20b) and (13) into Eq.

(28) yields

$$n(z)=\frac{\mathrm{Bu}}{2\pi i}\left[B\left(1-\frac{(1-k)}{X(z)}\right)-\frac{a_{0+}\nu_0}{2g(\nu_0)(\nu_0-z)}\times\left(1-\frac{X(\nu_0)}{X(z)}\right)-\frac{ka_{1+}\nu_1}{2g(\nu_1)(\nu_1-z)}\left(1-\frac{X(\nu_1)}{X(z)}\right)\right], \quad (29)$$

where we have used the identity

$$X(z)=\frac{1}{\mathrm{Bu}}\int_0^{1/\mathrm{Bu}}\frac{\gamma(\tilde{\mu})\,d\tilde{\mu}}{\tilde{\mu}-z}+(1-k). \quad (30)$$

Equation (30) can easily be proved by a procedure similar to that used in Ref. 11. It is required that the function $n(z)$ given by Eq. (29) has property (ii). For this purpose, we shall discuss the cases of $\beta\leq\beta_c$ and $\beta>\beta_c$ separately.

(i) The case $\beta\leq\beta_c$ $(k=1)$: In order that $n(z)$ vanish at infinity, property (ii) from Eq. (29), it is required that

$$B+\frac{a_{0+}\nu_0\mathrm{Bu}X(\nu_0)}{2g(\nu_0)}+\frac{a_{1+}\nu_1\mathrm{Bu}X(\nu_1)}{2g(\nu_1)}=0, \quad (31)$$

which is obtained by expanding Eq. (29) for large z and making use of the fact that

$$\lim_{z\to\infty}X(z)=1/(-\mathrm{Buz})^k, \quad (32)$$

which follows from Eq. (26). Thus, the function $n(z)$ given by Eq. (29) with the condition (31) satisfies properties (i) and (ii). It follows from Eqs. (23b) and (29) that

$$A(\nu)=j(\nu)\left(\frac{a_{0+}\nu_0X(\nu_0)}{2g(\nu_0)(\nu_0-\nu)}+\frac{a_{1+}\nu_1X(\nu_1)}{2g(\nu_1)(\nu_1-\nu)}\right), \quad (33a)$$

where

$$j(\nu)\equiv-\frac{[\mathrm{Bu}^2(\nu_1^2-\nu^2)]^k(\nu_0^2-\nu^2)X(-\nu)i\beta}{\Lambda^+(\nu)\Lambda^-(\nu)(\zeta^2-\nu^2)(1+i\beta)}. \quad (33b)$$

In arriving at Eq. (33b), we have made use of the identity

$$X(z)X(-z)=\frac{\Lambda(z)(\zeta^2-z^2)[1+(1/i\beta)]}{(\nu_0^2-z^2)[\mathrm{Bu}^2(\nu_1^2-z^2)]^k}. \quad (34)$$

The proof of Eq. (34) is, again, similar to analogous results given in Ref. 11. Equations (31) and (33a) are two of the three relations for the determination of a_{0+}, a_{1+}, and $A(\nu)$. The third relation can be obtained by imposing boundary condition (3) on Eq. (17) to yield

$$\frac{a_{0+}\nu_0X(\nu_0)h(\nu_0)}{2g(\nu_0)}+\frac{a_{1+}\nu_1X(\nu_1)h(\nu_1)}{2g(\nu_1)}=A, \quad (35a)$$

where

$$h(\nu_j)\equiv\tfrac{1}{2}i\gamma^{1/2}\times\left(\frac{1}{[\nu_j-(i/\gamma^{1/2})X(i/\gamma^{1/2})}-\frac{1}{[\nu_j+(i/\gamma^{1/2})X(-i/\gamma^{1/2})}\right), \quad j=1,2, \quad (35b)$$

and we have made use of Eqs. (22) and (29).

Solving Eqs. (31), (33a), and (35a), we have

$$a_{0+}=\frac{2g(\nu_0)[A\mathrm{Bu}+Bh(\nu_1)]}{\nu_0X(\nu_0)\mathrm{Bu}[h(\nu_0)-h(\nu_1)]}, \quad (36a)$$

$$a_{1+}=-\frac{2g(\nu_1)[A\mathrm{Bu}+Bh(\nu_0)]}{\nu_1X(\nu_1)\mathrm{Bu}[h(\nu_0)-h(\nu_1)]}, \quad (36b)$$

and

$$A(\nu)=j(\nu)\times\left(\frac{A\mathrm{Bu}(\nu_1-\nu_0)+B[(\nu_1-\nu)h(\nu_1)-(\nu_0-\nu)h(\nu_0)]}{\mathrm{Bu}(\nu_0-\nu)(\nu_1-\nu)[h(\nu_0)-h(\nu_1)]}\right). \quad (36c)$$

Thus the coefficients a_{0+}, a_{1+}, and $A(\nu)$ are uniquely determined.

(ii) The case when $\beta>\beta_c$ $(k=0)$: We now determine the coefficients a_{0+} and $A(\nu)$ for the case of $\beta>\beta_c$. First, we note that, with the aid of Eq. (32), it is easy to see that the function $n(z)$ given by Eq. (29) does vanish at infinity. Thus property (ii) is indeed satisfied. If we impose boundary condition (3) on Eq. (17) and make use of Eq. (31), we have

$$a_{0+}=\frac{2g(\nu_0)}{\nu_0X(\nu_0)h(\nu_0)}\times\left[A-\frac{i\gamma^{1/2}}{2}\left(\frac{1}{X(-i/\gamma^{1/2})}-\frac{1}{X(i/\gamma^{1/2})}\right)B\right]. \quad (37a)$$

The coefficient $A(\nu)$ can then be obtained from Eq. (23b) with the aid of Eqs. (29) and (37a) to give

$$A(\nu)=j(\nu)\left\{-B+\frac{1}{h(\nu_0)(\nu_0-\nu)}\times\left[A-\frac{i\gamma^{1/2}}{2}\left(\frac{1}{X(-i/\gamma^{1/2})}-\frac{1}{X(i/\gamma^{1/2})}\right)B\right]\right\}. \quad (37b)$$

Equations (16) and (17), with coefficients given by Eqs. (36) and (37), are the solution of this problem. Thus, the exact solution can be obtained by integration of quadratures.

IV. EXPLICIT EXPRESSIONS FOR DISTURBANCES AT THE GAS–SOLID INTERFACE

Simplified expressions can be obtained for all disturbed quantities at the gas–solid interface. The disturbed radiation intensity incident on the wall is given

by

$$\frac{\partial I'}{\partial t}(0,\mu,t)=\frac{4\sigma T_\infty^4}{\pi}\omega\left[a_{0+}\psi_{\nu_0}(\mu)+ka_{1+}\psi_{\nu_1}(\mu)+\frac{2\pi i}{\mathrm{Bu}}n\left(\frac{\mu}{\mathrm{Bu}}\right)\right]\exp(i\omega t),\qquad -1<\mu<0,\quad (38)$$

where we have used Eqs. (13) and (22). The disturbed average radiation intensity and the radiative heat flux are given by

$$\frac{\partial I_0'}{\partial t}(0,t)=8\sigma T_\infty^4\omega\left\{a_{0+}+ka_{1+}+\frac{2\pi(i-\beta)(\gamma\zeta^2+1)}{\mathrm{Bu}}\times\left[n\left(\frac{i}{\gamma^{1/2}}\right)+n\left(-\frac{i}{\gamma^{1/2}}\right)\right]-\frac{4\pi(i-\beta)\gamma\zeta^2 n(0)}{\mathrm{Bu}}\right\}\exp(i\omega t),\quad (39)$$

$$\frac{\partial q'}{\partial t}(0,t)=8\sigma T_\infty^3\omega\left\{a_{0+}\nu_0\mathrm{Bu}\left(1-\frac{1}{g(\nu_0)}\right)+ka_{1+}\nu_1\mathrm{Bu}\left(1-\frac{1}{g(\nu_1)}\right)-i\mathrm{Bu}\beta\frac{a_{0+}\nu_0}{g(\nu_0)}\times[1-X(\nu_0)-X(\nu_0)\mathrm{Bu}(\nu_0+d)]-i\mathrm{Bu}\beta\frac{ka_{1+}\nu_1}{g(\nu_1)}\times[1-X(\nu_1)-X(\nu_1)\mathrm{Bu}(\nu_1+d)]-2\pi\gamma^{1/2}(1+i\beta)\left(\zeta^2+\frac{1}{\gamma}\right)\times\left[n\left(\frac{i}{\gamma^{1/2}}\right)-n\left(-\frac{i}{\gamma^{1/2}}\right)\right]\right\}\exp(i\omega t),\quad (40a)$$

where

$$d\equiv\frac{1}{2\pi i}\int_0^{1/\mathrm{Bu}}\ln\left(\frac{\Lambda^+(\tilde{\mu})}{\Lambda^-(\tilde{\mu})}\right)d\tilde{\mu}.\quad (40b)$$

With some manipulation, the disturbed velocity potential, pressure, density, and temperature at the gas–solid interface are given by

$$\phi(0,t)=\frac{ip'}{\omega\rho_\infty}(0,t)=\frac{RT_\infty}{\omega}\left\{\frac{a_{0+}}{2g(\nu_0)(1+1/\gamma\nu_0^2)}+\frac{ka_{1+}}{2g(\nu_1)(1+1/\gamma\nu_1^2)}+\frac{\pi i}{\mathrm{Bu}}\left[n\left(\frac{i}{\gamma^{1/2}}\right)+n\left(-\frac{i}{\gamma^{1/2}}\right)\right]\right\}\times\exp(i\omega t),\quad (41)$$

$$\frac{\partial\rho'}{\partial t}(0,t)=-\frac{\omega\rho_\infty}{\gamma}\left\{\frac{a_{0+}}{2g(\nu_1)(1+1/\gamma\nu_0^2)\nu_0^2}+\frac{ka_{1+}}{2g(\nu_1)(1+1/\gamma\nu_1^2)\nu_1^2}+\frac{i\pi\gamma}{\mathrm{Bu}}\times\left[2n(0)-n\left(\frac{i}{\gamma^{1/2}}\right)-n\left(-\frac{i}{\gamma^{1/2}}\right)\right]\right\}\exp(i\omega t),\quad (42)$$

and

$$\frac{\partial T'}{\partial t}(0,t)=\omega T_\infty\left(\frac{a_{0+}}{2g(\nu_0)}+\frac{ka_{1+}}{2g(\nu_1)}+\frac{2\pi i n(0)}{\mathrm{Bu}}\right)\exp(i\omega t).\quad (43)$$

It is worth noting that the temperature of the gas adjacent to the wall as given by Eq. (43) differs from that of the wall as given by Eq. (4a). In the literature the difference is referred to as the radiation slip.[17]

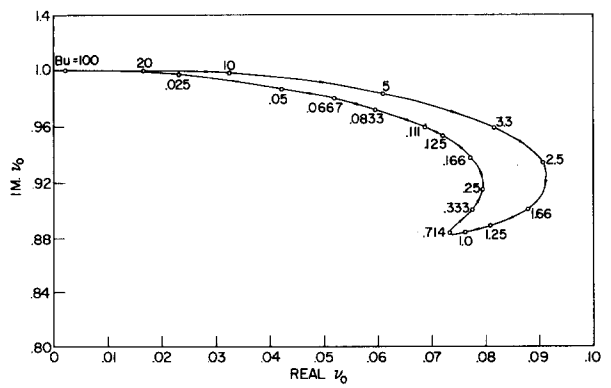

FIG. 1. The first discrete root (ν_0) of $\Lambda(\nu)=0$ (Bo=3.23, $\gamma=1.4$).

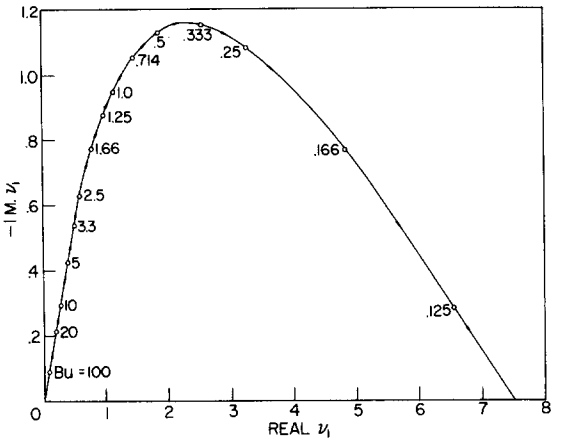

FIG. 2. The second discrete root (ν_1) of $\Lambda(\nu)=0$ (Bo=3.23, $\gamma=1.4$).

V. DISCUSSION OF NUMERICAL RESULTS

In order to assess the accuracy of the differential approximation, the disturbances at the gas–solid interface ($\xi=0$) as obtained from the exact solution and that of the differential approximation (with the Mark and Marshak boundary conditions) were computed. Calculations were carried out for Bo=3.23 and $\gamma=1.4$ for the range of Bouguer numbers (Bu) from 0.01

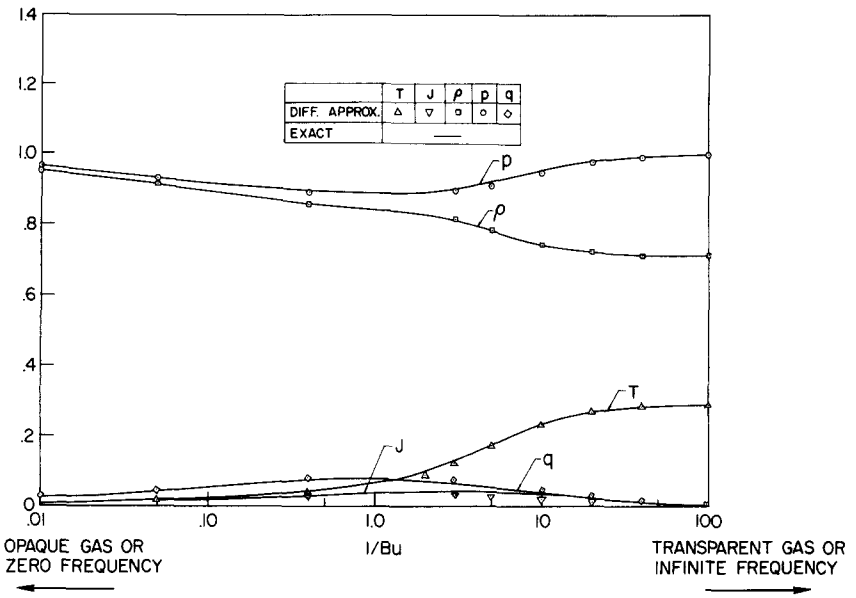

FIG. 3. Comparison of the amplitudes of disturbances (at $\xi=0$) for pure wall motion, as obtained from the exact solution and the differential approximation (Bo=3.23, $\gamma=1.4$).

(transparent) to 100 (opaque) for the cases of pure wall motion ($A=1, B=0$) and pure wall temperature variation ($A=0, B=1$). The results of the computations are presented in Figs. 1–11, where the amplitudes of the disturbances are expressed in terms of dimensionless quantities, i.e., $p=p'/p_\infty$, $T=T'/T_\infty$, $\rho=\rho'/\rho_\infty$, $I=I'(4\sigma T_\infty{}^4/\pi)^{-1}$, $q=q'/4\sigma T_\infty{}^4$, and $J=I_0'/16\sigma T_\infty{}^4$. For future reference, some of the representative results are also tabulated in Table I.

Figures 1 and 2 show the discrete roots (ν_j) of Eq. (11). The physical meaning of the roots will be apparent if we let $1/\nu_j=\delta_j+i\lambda_j$, where δ_j is the damping factor and a_s/λ_j is the wave speed. It is shown (Fig. 1) that the first discrete root (ν_0) starts from the imaginary number i with the real part of ν_0 increasing from zero and returning back to zero as Bu decreases from ∞ to 0. Thus for the cases of Bu$\to\infty$ and Bu=0, the damping factor is zero and the wave speed is a_s. The wave asso-

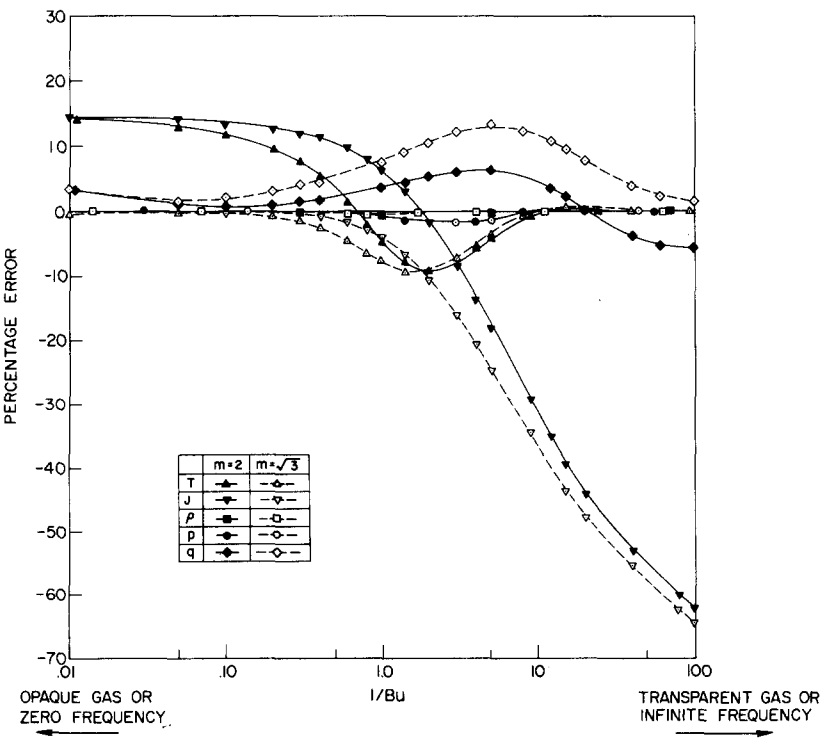

FIG. 4. Percentage of error of the differential approximation with the Marshak ($m=2$) and the Mark ($m=\sqrt{3}$) boundary conditions for pure wall motion as a function of Bu (Bo=3.23, $\gamma=1.4$).

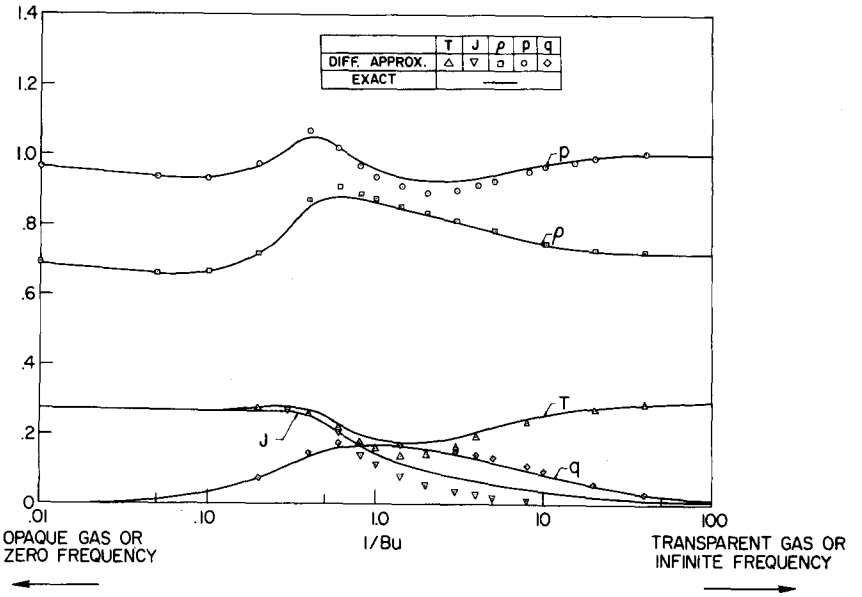

FIG. 5. Amplitude of the modified classical wave (at $\xi=0$) for pure wall motion (Bo=3.23, $\gamma=1.4$).

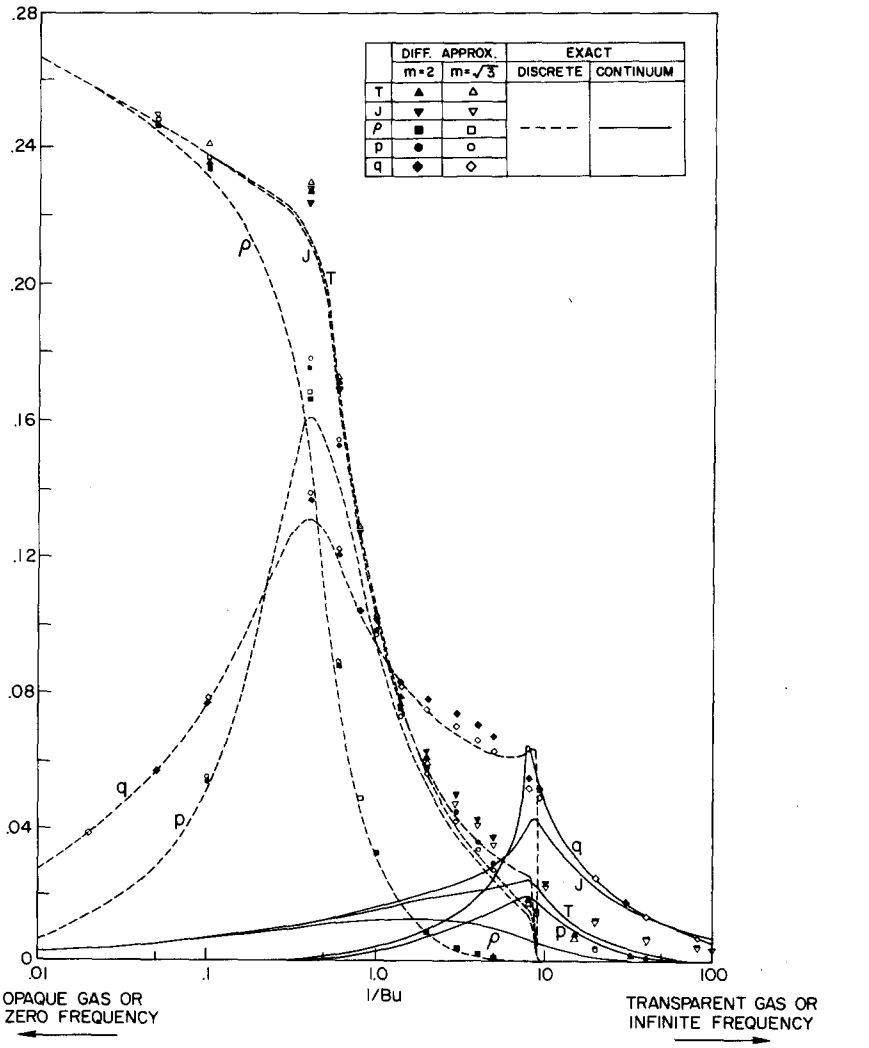

FIG. 6. Amplitude of the radiation-induced wave (at $\xi=0$) for pure wall motion (Bo=3.23, $\gamma=1.4$).

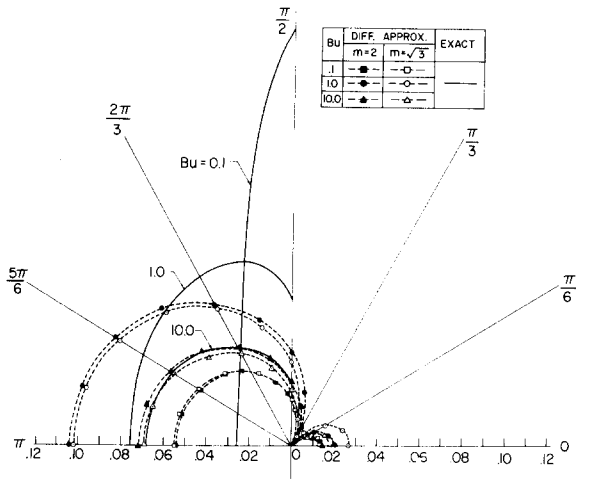

FIG. 7. Comparison of the amplitude of the radiation intensity (at $\xi=0$) in polar coordinates for pure wall motion, as obtained from the exact solution and the differential approximation (Bo=3.23, $\gamma=1.4$).

ciated with the discrete root ν_0 can therefore be identified as the modified classical wave.[1] The value of the second root ν_1 is strongly dependent on Bu, as is evident from Fig. 2. As Bu decreases from ∞ to the critical Bouguer number Bu_c ($Bu_c=0.1107$ for Bo=3.23 and $\gamma=1.4$, which is obtained as discussed in Appendix A), the value of ν_1 changes from 0 (i.e., damping factor $\delta_1\to\infty$ and wave speed 0) to the real number 7.5 (i.e., damping factor $\delta_1=0.133$ and wave speed ∞). The root ν_1 disappears for $Bu<Bu_c$.

The amplitudes of the disturbances depend on the boundary conditions. Figures 3–7 show the amplitudes of disturbances at the gas–solid interface for pure wall motion, whereas Figs. 8–11 show the corresponding results for pure wall temperature variations.

The comparison of the amplitudes of disturbances at the gas–solid interface for pure wall motion, as obtained from the exact solution and that of the differential approximation, are shown in Fig. 3. Since the difference between values obtained based on the Mark and Marshak boundary conditions is negligible, they are undiscernible in this plot. The temperature slip is shown to be zero for an opaque gas and increases as Bu increases. The emission of the gas (as represented by T) and the absorption of the gas (as represented by J) are shown to be equal for an opaque gas, and the effect of emission becomes dominating as 1/Bu increases. This is in support of the assertion that absorption is negligible compared with emission for a thin gas without external radiation.

The percentage of error of the differential approximation with the Mark and Marshak boundary conditions for pure wall motion is shown in Fig. 4. It is shown that, with the exception of J, the error in the differential approximation is within 15%, with maximum error in the neighborhood of $Bu\cong 0.2$–1.0, and approaches zero at the limits of $Bu\to 0$ and $Bu\to\infty$.

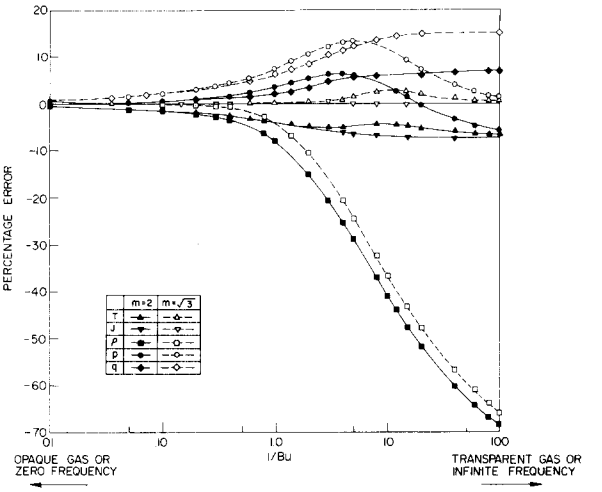

FIG. 9. Percentage of error of the differential approximation with the Marshak ($m=2$) and the Mark ($m=\sqrt{3}$) boundary conditions for pure wall temperature variations (Bo=3.23, $\gamma=1.4$).

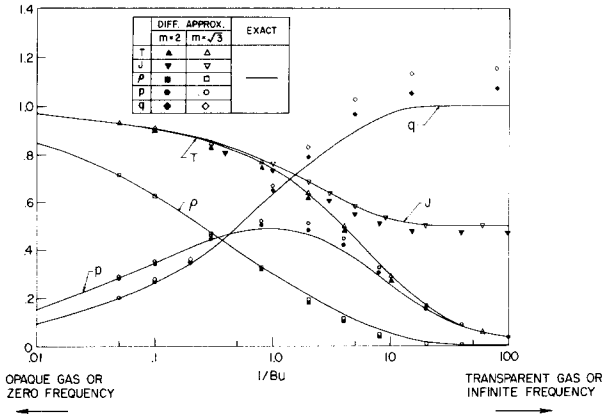

FIG. 8. Comparison of the amplitudes of disturbances (at $\xi=0$) for pure wall temperature variations, as obtained from the exact solution and the differential approximation (Bo=3.23, $\gamma=1.4$).

The contributions of the modified classical wave and the radiation-induced wave to the total disturbances are shown, respectively, in Figs. 5 and 6. As shown in Fig. 5, the differential approximation predicts the modified classical wave reasonably well; the differences between those based on the Marshak and Mark conditions are indistinguishable in this plot. The amplitude of the radiation-induced wave is shown in Fig. 6, where it should be noted that the exact solution consists of both the discrete mode (associated with ν_1) and the continuum mode. The amplitude of the discrete mode is shown to be much larger than the continuum mode for $Bu>Bu_c$ ($1/Bu_c=9.035$) and disappears for $Bu<Bu_c$. With the exception of ρ, the maximum amplitude of the continuum mode occurs near the critical Bouguer number. In this figure, it is noted that the differential approximation predicts the

TABLE I. Amplitude of disturbances at the gas–solid interface as obtained from the exact solution and the differential approximation.

Bu	$\lvert p \rvert$			$\lvert \rho \rvert$			$\lvert T \rvert$			$\lvert q \rvert$			$\lvert J \rvert$		
	Exact	Diff. approx.		Exact	Diff. approx.		Exact	Diff. approx.		Exact	Diff. approx.		Exact	Diff. approx.	
		$m=2$	$m=\sqrt{3}$		$m=2$	$m=\sqrt{3}$		$m=2$	$m=\sqrt{3}$		$m=2$	$m=\sqrt{3}$		$m=2$	$m=\sqrt{3}$
							Pure Wall Motion								
100	0.9666	0.9658	0.9657	0.9580	0.9559	0.9571	0.01137	0.01295	0.01132	0.02449	0.02520	0.02532	0.01102	0.01260	0.01096
10	0.9180	0.9177	0.9168	0.8951	0.8914	0.8938	0.02812	0.03142	0.02802	0.05720	0.05765	0.05847	0.02535	0.02882	0.02532
2.5	0.8931	0.8920	0.8897	0.8578	0.8524	0.8543	0.04441	0.04675	0.04320	0.07597	0.07730	0.07937	0.03467	0.03865	0.03437
1.0	0.8887	0.8855	0.8827	0.8420	0.8372	0.8382	0.06569	0.06252	0.06066	0.08012	0.08297	0.08627	0.03892	0.04150	0.03735
0.5	0.8939	0.8873	0.8850	0.8273	0.8255	0.8256	0.1002	0.09106	0.09122	0.07610	0.08022	0.08432	0.04077	0.04010	0.03650
0.2	0.9211	0.9116	0.9112	0.7849	0.7862	0.7859	0.1785	0.1710	0.1722	0.06015	0.06385	0.06810	0.03885	0.03192	0.02947
0.025	0.9945	0.9953	0.9954	0.7168	0.7168	0.7168	0.2805	0.2814	0.2815	0.01352	0.01306	0.01406	0.01378	0.00656	0.00612
0.01	0.9989	0.9992	0.9992	0.7147	0.7147	0.7147	0.2847	0.2850	0.2850	0.00561	0.00530	0.00571	0.00710	0.00269	0.00251
							Pure Temperature Variation								
100	0.1528	0.1529	0.1536	0.8542	0.8501	0.8543	0.9690	0.9643	0.9689	0.09662	0.09660	0.09705	0.9690	0.9642	0.9690
10	0.3473	0.3498	0.3549	0.6246	0.6148	0.6238	0.9083	0.8953	0.9083	0.2658	0.2678	0.2718	0.9093	0.8962	0.9092
2.5	0.4610	0.4691	0.4817	0.4266	0.4117	0.4227	0.8290	0.8072	0.8289	0.4580	0.4648	0.4773	0.8345	0.8130	0.8350
1.0	0.4861	0.5036	0.5235	0.3003	0.2771	0.2881	0.7402	0.7122	0.7403	0.6283	0.6430	0.6683	0.7575	0.7302	0.7590
0.5	0.4618	0.4867	0.5117	0.2162	0.1842	0.1936	0.6394	0.6092	0.6405	0.7660	0.7918	0.8323	0.6833	0.6520	0.6855
0.2	0.3650	0.3875	0.4133	0.1135	0.08083	0.08620	0.4469	0.4249	0.4531	0.9130	0.9615	1.026	0.5825	0.5470	0.5835
0.025	0.08203	0.07922	0.08533	0.00600	0.00244	0.00263	0.08444	0.07941	0.08553	0.9984	1.069	1.151	0.5024	0.4663	0.5023
0.01	0.03402	0.03210	0.03458	0.00124	0.00040	0.00043	0.03441	0.03211	0.03459	0.9997	1.071	1.154	0.5004	0.4644	0.5003

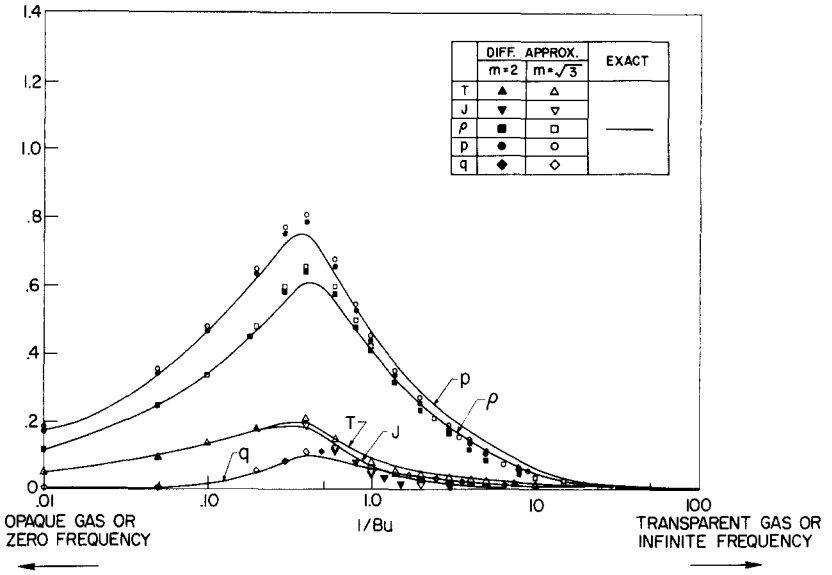

FIG. 10. Amplitude of the modified classical wave (at $\xi=0$) for pure wall temperature variations (Bo=3.23, $\gamma=1.4$).

radiation-induced wave in an approximate manner: for $Bu>Bu_c$ the exponential term in the differential approximation represents the combination of the discrete mode and the continuum mode, whereas for $Bu<Bu_c$, where the discrete mode of the exact solution disappears, the exponential term in the differential approximation approximates the continuum mode. The amplitude of the radiation-induced wave based on the Mark boundary condition differs somewhat from that of the Marshak boundary condition, as is shown in Fig. 6.

The amplitude of the radiation intensity (at $\xi=0$) in polar coordinate for pure wall motion is shown in Fig. 7. Since the radiation intensity is symmetric with respect to $\theta=0$ and $\theta=\pi$, only the portion with $0\leq\theta\leq\pi$ is plotted. For the exact solution, it is shown that the radiation intensity is discontinuous at $\theta=\frac{1}{2}\pi$ and that its value is zero (because of zero wall temperature) for $0\leq\theta\leq\frac{1}{2}\pi$; the radiation intensity is very anisotropic for Bu=0.1 and becomes more isotropic as Bu increases. The differential approximation, however, predicts erroneously that the radiation intensity is continuous at $\theta=\frac{1}{2}\pi$ and is nonzero for $0\leq\theta\leq\frac{1}{2}\pi$.

Figure 8 shows the amplitude of disturbances at the gas–solid interface for pure wall temperature variation. It is shown that the emission is equal to the absorption for an opaque gas and the effect of absorption becomes

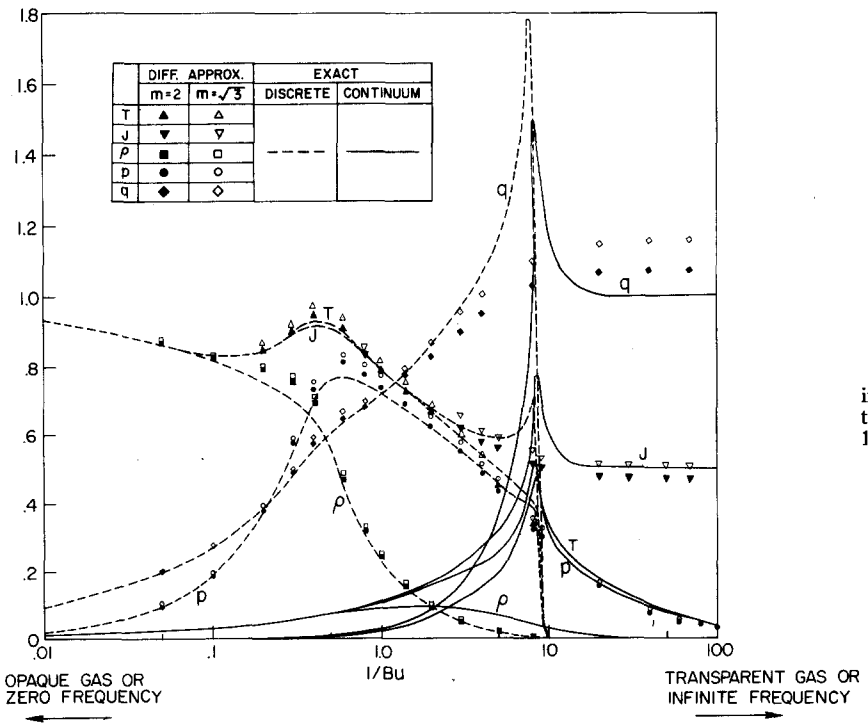

FIG. 11. Amplitude of the radiation-induced wave (at $\xi=0$) for pure wall temperature variations (Bo=2.23, $\gamma=1.4$).

dominating as 1/Bu increases. This is in support of the assertion that the thin gas approximation with the effect of absorption being neglected would be in serious error when external radiation exists.[14] Again, the radia-slip is shown to be zero for an opaque gas, and its value increases as 1/Bu increases. The amplitude of disturbances (for pure wall temperature variations) obtained based on the Mark boundary condition differs somewhat from those of the Marshak boundary condition.

The percentage error in the differential approximation with the Mark and the Marshak boundary conditions for pure wall temperature variations is shown in Fig. 9, where it is shown that the error is zero for an opaque gas and, in general, increases as 1/Bu increases. With the exception of ρ, the maximum error is within 15%.

The contributions of the modified classical wave and the radiation-induced wave to the total disturbances for pure wall temperature variation are plotted in Figs. 10 and 11. For the modified classical wave, the maximum values of disturbances occur near Bu$\sim$2; the differences between the values obtained with the Mark boundary condition and those of the Marshak boundary condition are small but not undiscernible. The amplitude of the radiation-induced wave is shown in Fig. 11, where it is noted that the exact solution consists of the continuum mode and a discrete mode, with the discrete mode vanishing for $\mathrm{Bu}<\mathrm{Bu}_c$. For $\mathrm{Bu}>\mathrm{Bu}_c$, the amplitude of the discrete mode is much larger than that of the continuum mode; this situation becomes reversed in the neighborhood of Bu_c, where the amplitude of the discrete mode is smaller than the continuum mode.

VI. CONCLUDING REMARKS

From the above discussion, several conclusions can now be made.

(1) The exact analysis shows that the disturbances, in general, consist of two discrete modes and a continuum mode. The continuum mode of disturbances had not been found in previous analyses.

(2) As Bu decreases from ∞ to 0, the wave speed of one of the discrete modes (i.e., ν_0) varies from a_s to $a_s/\gamma^{1/2}$ and back to a_s with damping increasing from 0 to a small amount and then decreasing to 0 (Fig. 1). Since this mode of disturbance has slight damping and a wave speed not much different from the isentropic speed of sound, it can be identified as the so-called modified classical wave.

(3) The other discrete mode (ν_1) depends strongly on the Bouguer number and disappears when $\mathrm{Bu}<\mathrm{Bu}_c$. As Bu decreases from ∞ to Bu_c, the damping factor decreases from ∞ to a small number while the wave speed increases from 0 to infinity (Fig. 2). Since this wave has no counterpart in classical theory, it is, therefore, radiation induced.

(4) The continuum mode with infinite wave speed and with damping in the range of ∞ to Bu is also radiation induced. This mode of disturbances, is, therefore, highly damped when Bu is large.

(5) The relative amplitudes of the modified classical wave (consisting of a discrete mode) and the radiation-induced wave (consisting of a discrete mode and a continuum mode) depend on the boundary conditions as well as the particular range of Bu considered. The amplitude of the continuum mode, however, is always zero for a sufficiently thick gas regardless of boundary conditions.

(6) The differential approximation predicts the modified classical wave reasonably well while it predicts the radiation-induced wave in an approximate manner. The exponential term in the differential approximation represents the combination of the discrete mode and the continuum mode for $\mathrm{Bu}>\mathrm{Bu}_c$, whereas it represents the continuum mode when $\mathrm{Bu}<\mathrm{Bu}_c$.

(7) Although the discrete mode of the radiation-induced wave is discontinuous at $\mathrm{Bu}=\mathrm{Bu}_c$, the total disturbances are smooth near the critical Bouguer number. For this reason, it appears that the value of the critical Bouguer number may not be found experimentally.

(8) The differences in numerical results based on the Mark and the Marshak boundary conditions for the differential approximation are negligible for problems without external radiation; they become somewhat larger for problems with external radiation. The Mark boundary condition appears to be more accurate for the determination of T, ρ, and J, whereas the Marshak boundary condition is better for q and p. Thus, for problems where radiative heat flux is of primary interest, the Marshak boundary condition should be used.

(9) When external radiation is unimportant, the differential approximation is within a 15% error for all variables (except J), with maximum error occurring in the range of Bu$\cong$0.2–1.0. For problems with external radiation, the error in the differential approximation is also within 15% for all variables except density, which is rather inaccurate; the error in the differential approximation increases as 1/Bu increases.

These conclusions are drawn from numerical results based on one specific value of Bo (i.e., Bo=3.23). It is expected that they hold for other values of Bo. For a quantitative comparison of the differential approximation and the exact solutions for large values of Bo, see also Ref. 18.

ACKNOWLEDGMENTS

The authors wish to thank M. W. Rubesin and B. S. Baldwin, Jr., for their interest. They also wish to thank E. Williams for her capable assistance in the numerical work. For the case of the first author (P.C.), the work was carried out while he was pursuing a National Academy of Science–National Research Council resident associateship.

APPENDIX A: NUMBER OF ZEROS OF THE FUNCTION $\Lambda(\nu)$

Except for two poles at the zeros of $g(\nu)$, the function $\Lambda(\nu)$ given by Eq. (11) is analytic in the complex plane

of ν cut along $(-1/\mathrm{Bu}, 1/\mathrm{Bu})$. To find the number of zeros of $\Lambda(\nu)$, it is more convenient to consider the function $\Omega(\nu)$ given by

$$\Omega(\nu)=[(\nu^2+\gamma^{-1})+i\beta(\nu^2+1)]\Lambda(\nu), \tag{A1}$$

which has the same roots as $\Lambda(\nu)$ but has no poles.

By the principle of the argument,[19] we have

$$N_z-N_p=(2\pi)^{-1}\Delta \arg\Omega(\nu)|_C, \tag{A2}$$

where $\Delta \arg\Omega(\nu)|_C$ denotes the change in argument of $\Omega(\nu)$ around a closed contour C within which the function is analytic except for the poles. N_z and N_p are, respectively, the number of zeros and number of poles of the function $\Omega(\nu)$ within the closed contour C consisting of segments $C_1^{\pm}$, C_1', and C_1'', and circular contours C_R and $C_\rho^{\pm}$ (see Fig. 12). If the function $\Omega(\nu)$ as given by Eq. (A1) is expanded for large ν, it is easy to show that this function is constant along C_∞ $(R\to\infty)$ so that the change in argument of $\Omega(\nu)$ along this path is zero. Along the remaining contours $C_1^{\pm}$, we have

$$\begin{aligned}(2\pi)^{-1}&\Delta \arg\Omega(\nu)|_{C_1^+ + C_1^-}\\ &=(2\pi)^{-1}[\theta_1(1/\mathrm{Bu})-\theta_1(-1/\mathrm{Bu})]\\ &\quad-(2\pi)^{-1}[\theta_2(1/\mathrm{Bu})-\theta_2(-1/\mathrm{Bu})],\end{aligned} \tag{A3}$$

where

$$\theta_{1,2}(\nu)\equiv \arg\Omega^{\pm}(\nu)$$

$$=\tan^{-1}\left(\frac{\beta(\nu^2+1)\pm\frac{1}{2}[\pi\mathrm{Bu}\nu(\nu^2+\gamma^{-1})]}{(\nu^2+\gamma^{-1})[1-\frac{1}{2}(\mathrm{Bu}\nu)\ln(1+\mathrm{Bu}\nu)/(1-\mathrm{Bu}\nu)]}\right). \tag{A4}$$

Since $\theta_1(\nu)=\theta_2(-\nu)\pm 2n\pi$, it follows from Eq. (A3) that

$$(2\pi)^{-1}\Delta \arg\Omega(\nu)|_{C_1^+ + C_1^-}=\pi^{-1}[\theta_1(1/\mathrm{Bu})-\theta_1(-1/\mathrm{Bu})], \tag{A5}$$

where $\theta_1(1/\mathrm{Bu})=\pi$ and the value of $\theta_1(-1/\mathrm{Bu})$ depends on the value of β as follows. Suppose that the real part of $\Omega^+(\nu)$, i.e., the denominator of $\tan\theta(\nu)$ vanishes at ν^* whereas the imaginary part of $\Omega^+(\nu)$, i.e., the nominator of $\tan\theta(\nu)$, vanishes at $\tilde{\nu}$. For a specific value of Bu, there is a value β such that $\nu^*=\tilde{\nu}$. We shall refer to this particular value of β as β_c. It is apparent by a numerical evaluation that:

(i) If $\beta<\beta_c$, then $|\nu^*|>|\tilde{\nu}|$ and $\theta(-1/\mathrm{Bu})=-\pi$, and

(ii) if $\beta>\beta_c$, then $|\nu^*|<|\tilde{\nu}|$ and $\theta(-1/\mathrm{Bu})=\pi$.

We conclude therefore that, if $\beta\le\beta_c$, then

$$(1/2\pi)\Delta \arg\Omega(\nu)|_{C_1^+ + C_1^-}=2$$

and the function $\Lambda(\nu)$ has four zeros, whereas for $\beta>\beta_c$, then $(1/2\pi)\Delta \arg\Omega(\nu)|_{C_1^+ + C_1^-}=0$ and the function $\Lambda(\nu)$ has two zeros. For the special case of $\beta=\beta_c$, one of the four roots is at $\nu=-\nu^*$ on the top of the cut while another root is at $\nu=\nu^*$ on the bottom of the cut.

APPENDIX B: DERIVATION OF $X(z)$

The function $X(z)$, given by Eq. (26), is analytic in the complex plane cut from 0 to 1/Bu; its boundary values satisfy the ratio condition

$$X^+(\mu)/X^-(\mu)=\Lambda^+(\mu)/\Lambda^-(\mu), \tag{B1}$$

and it is nonvanishing in the finite cut plane.

Proof: It follows from the Plemelj formulas that the boundary values of (B1) are given by

$$X^{\pm}(\mu)=\frac{1}{(1-\mathrm{Bu}\mu)^k}\times\exp\left[\frac{P}{2\pi i}\int_0^{1/\mathrm{Bu}}\ln\left(\frac{\Lambda^+(\tilde{\mu})}{\Lambda^-(\tilde{\mu})}\right)\frac{d\tilde{\mu}}{\tilde{\mu}-\mu}\pm\frac{1}{2}\ln\left(\frac{\Lambda^+(\mu)}{\Lambda^-(\mu)}\right)\right], \tag{B2}$$

from which it is easily seen that X^+ and X^- satisfy (B1). To verify that $X(z)$ is nonvanishing, note that the values of $z=0$ and $z=1/\mathrm{Bu}$ are the only points where the integral in Eq. (26) has the possibility of being infinite. At other points along the cut, for example, the principal value integral is bounded. At the point $z=0$, the integral is bounded since we can take $\ln[\Lambda^+(0)/\Lambda^-(0)]=0$. Near $z=1/\mathrm{Bu}$, Eq. (26) can be written as

$$X(z)=\frac{1}{(-\mathrm{Buz})^k}\times\exp\left[\frac{1}{2\pi i}\int_0^{1/\mathrm{Bu}}\left(\ln\frac{\Lambda^+(\mu)}{\Lambda^-(\mu)}-\ln\frac{\Lambda^+(1/\mathrm{Bu})}{\Lambda^-(1/\mathrm{Bu})}\right)\frac{d\mu}{\mu-z}\right], \tag{B3}$$

from which it may be verified that $X(z)$ has only logarithmic behavior at $z=1/\mathrm{Bu}$.

APPENDIX C: APPROXIMATE SOLUTION BASED ON THE DIFFERENTIAL APPROXIMATION

The disturbed velocity potential for this problem, based on the differential approximation, was obtained elsewhere.[1,2] For completeness here we collect the results that have been used for computation in Sec. V.

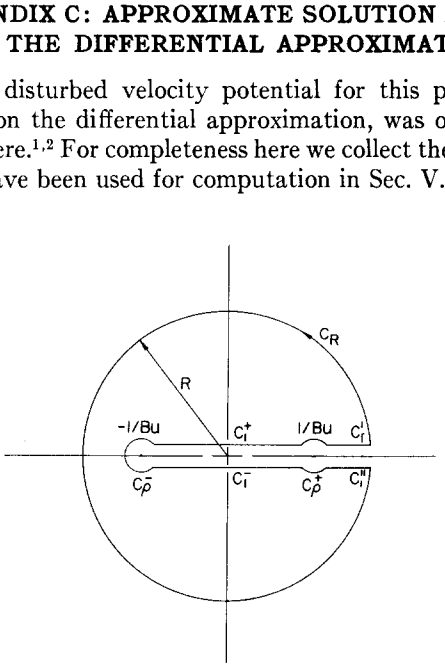

FIG. 12. Sketch of the contour for Eq. (A4).

The disturbed velocity potential is[1,2]

$$\phi(\xi, t) = \frac{RT_\infty}{\omega} \sum_{j=0}^{1} A_j \exp\left(-\frac{\xi}{\nu_j} + i\omega t\right), \quad \text{(C1)}$$

where ν_j's are the roots determined from

$$\left(1+\frac{1}{\nu_j^2}\right)\left(\frac{1}{\nu_j^2}-3\mathrm{Bu}^2\right) - \frac{i}{\beta\nu_j^2}\left(1+\frac{1}{\gamma\nu_j^2}\right) = 0, \quad \text{(C2)}$$

and amplitudes A_0 and A_1 are given by

$$A_0 = -D^{-1}\left(\frac{\sqrt{3}\mathrm{Bu}(\gamma+1/\nu_1^2)(m/\sqrt{3}\nu_1+\sqrt{3}\mathrm{Bu})A}{\gamma(1/\nu_1^2-3\mathrm{Bu}^2)} - \frac{B}{\nu_1}\right) \quad \text{(C3)}$$

and

$$A_1 = D^{-1}\left(\frac{\sqrt{3}\mathrm{Bu}(\gamma+1/\nu_0^2)(m/\sqrt{3}\nu_0+\sqrt{3}\mathrm{Bu})A}{\gamma(1/\nu_0^2-3\mathrm{Bu}^2)} - \frac{B}{\nu_0}\right), \quad \text{(C4)}$$

where

$$D \equiv \frac{\sqrt{3}\mathrm{Bu}}{\gamma}\left(\frac{(\gamma+1/\nu_1^2)(m/\sqrt{3}\mathrm{Bu})}{\nu_0(1/\nu_1^2-3\mathrm{Bu}^2)} - \frac{(\gamma+1/\nu_0^2)(m/\sqrt{3}\nu_0+\sqrt{3}\mathrm{Bu})}{\nu_1(1/\nu_0^2-3\mathrm{Bu}^2)}\right), \quad \text{(C5)}$$

with $m=2$ for the Marshak boundary condition[2] and $m=\sqrt{3}$ for the Mark boundary condition,[2] and ν_0 and ν_1 denoting the roots of Eq. (C2) having positive real parts. The disturbances in the flow field (such as pressure, temperature, etc.) and in the radiation field (such as radiative heat flux) can then be obtained by the appropriate differentiation of the velocity potential. Within the differential approximation, the radiation intensity is given by

$$\frac{\partial I'}{\partial t}(\xi, \mu, t) = (4\pi)^{-1}\left(\frac{\partial I_0'}{\partial t}(\xi, t) + 3\mu\frac{\partial q'}{\partial t}(\xi, t)\right). \quad \text{(C6)}$$

* Present address: Department of Mechanical Engineering, University of Hawaii, Honolulu, Hawaii 96822.

[1] W. G. Vincenti and B. S. Baldwin, Jr., J. Fluid Mech. **12,** 449 (1962).
[2] P. Cheng, Ph.D. dissertation, Stanford University (1965).
[3] S. C. Traugott, in *Proceedings of the Heat Transfer and Fluid Mechanics Institute* (Stanford University Press, Stanford, California, 1963), p. 1.
[4] P. Cheng, AIAA J. **3,** 1662 (1964).
[5] P. Cheng, AIAA J. **4,** 236 (1966).
[6] P. Cheng and W. G. Vincenti, J. Fluid Mech. **27,** 625 (1967).
[7] W. E. Pearson, NASA TN D-2128 (1964).
[8] D. Finkleman and J. R. Baron, AIAA J. **8,** 87 (1970).
[9] M. C. Jischke and J. R. Baron, AIAA J. **7,** 1326 (1969).
[10] K. M. Case, Ann. Phys. (N.Y.) **9,** 1 (1960).
[11] K. M. Case and P. F. Zweifel, *Linear Transport Theory* (Addison-Wesley, Reading, Mass., 1967), Chap. 4.
[12] J. H. Ferziger and G. M. Simmons, Intern. J. Heat Mass Transfer **9,** 987 (1966).
[13] C. E. Siewert and P. F. Zweifel, Ann. Phys. (N.Y.) **36,** 61 (1966).
[14] W. G. Vincenti and C. H. Kruger, *Introduction to Physical Gasdynamics* (Wiley, New York, 1965), Chap. 7.
[15] K. M. Case, R. Zelazny, and M. Kanal, J. Math. Phys. **11,** 223 (1970).
[16] N. I. Muskhelishvili, *Singular Integral Equations* (Noordhoff, Groningen, The Netherlands, 1953), p. 42.
[17] R. F. Probstein, AIAA J. **1,** 1202 (1963).
[18] A. C. Cogley and D. L. Compton, Phys. Fluids **13,** 877 (1970).
[19] E. T. Copson, *Theory of Functions of a Complex Variable* (Oxford University Press, Oxford, 1955), p. 119.

THE PHYSICS OF FLUIDS VOLUME 14, NUMBER 5 MAY 1971

Flow of Rarefied Gas over Plane Wall

YOSHIO SONE AND KYOJI YAMAMOTO
Department of Aeronautical Engineering, Kyoto University, Kyoto, Japan
(Received 17 November 1969; final manuscript received 9 September 1970)

Flow of rarefied gas over an infinite plane wall on the basis of a relaxation model of the Boltzmann equation is considered. The solution is obtained in the form: Hilbert solution and boundary layer term which is appreciable only in a thin layer (with thickness of order of the mean free path) adjacent to the boundary. The Hilbert part dominates in the region away from the boundary. Using the result the asymptotic behavior (for small mean free path) of plane compressible Couette flow is investigated.

I. INTRODUCTION

In the flow of a slightly rarefied gas over a solid boundary, a thin layer (with thickness of order of the mean free path) appears adjacent to the boundary. The analysis of the layer has been treated as a flow over a flat wall by linearizing the problem using the assumption of a small variation in this layer[1–4] on the basis of a relaxation model of the Boltzmann equation.[1,5,6]

As the velocity of the outer flow increases, we can no longer linearize the problem even in the thin layer. In our previous paper[7] a treatment of the flow over a plane wall is given by taking into account the quantities of second order in flow velocity for the special case where temperature and density are uniform in the linearized problem. This condition, however, limits the applicability of the result to a large extent. Here, we analyze the flow of a rarefied gas over a plane wall more generally (for small Knudsen number but finite Mach number).

Finally, we investigate the asymptotic behavior (for small mean free path limit) of compressible Couette flow as a simple application of the theory.

II. FUNDAMENTAL EQUATION

We consider steady flow over a flat wall where the quantities do not change in the direction parallel to the